The Astrophysical Journal, 761:17 (6pp), 2012 December 10 doi:10.1088/0004-637X/761/1/17

THE LOCAL INTERSTELLAR SPECTRUM BEYOND THE HELIOPAUSE: WHAT CAN BE LEARNED FROM *VOYAGER* IN THE INNER HELIOSHEATH?

K. Herbst[1], B. Heber[1], A. Kopp[1], O. Sternal[1,3], and F. Steinhilber[2]
[1] IEAP, Christian-Albrechts-Universität zu Kiel, Leibnizstraße 11, D-24118 Kiel, Germany; herbst@physik.uni-kiel.de
[2] Swiss Federal Institute of Aquatic Science and Technology, Eawag, CH-8600 Dübendorf, Switzerland
Received 2011 August 11; accepted 2012 August 21; published 2012 November 20

ABSTRACT

The local interstellar spectrum (LIS) is one of the most important but unknown parameters used in all modeling efforts to describe the modulation of Galactic cosmic rays on their way from the galaxy through a possible bow shock, heliosheath, and heliosphere toward the Earth. Because it has not been measured thus far, several LIS models derived from numerical simulations or data on Earth were developed. A new method to determine the LIS was introduced when the *Voyager* spacecraft crossed the termination shock and entered the heliosheath. Webber & Higbie derived a new LIS, which is lower than all previous LIS models over the entire energy range, on the basis of these measurements. Numerical simulations by Scherer et al. showed that particles already in the outer heliosheath (OHS) are modulated, suggesting that the LIS by Webber & Higbie is a heliopause spectrum (HPS) rather than the "true" LIS. By using the same simplified simulation model, we estimate the diffusion coefficient in the OHS to be consistent with several 10^{26} to 10^{27} cm^2 s^{-1} for all LIS models under consideration by mapping them to this HPS and conclude that the *Voyager* measurements will not be able to determine the LIS in the near future. We then discuss the circumstances under which the terrestrial archive can be used to at least exclude LIS models, unless one awaits a dedicated mission like e.g., the *Interstellar Probe*.

Key words: acceleration of particles – astroparticle physics – Sun: heliosphere

Online-only material: color figures

1. INTRODUCTION

The three-dimensional region around the Sun controlled by the solar wind and its embedded magnetic field is called the heliosphere (see Figure 1, dark gray region). The interaction of the supersonic solar wind with the local interstellar medium (LISM) leads to a transition of the solar wind from supersonic to subsonic speeds at the termination shock (TS). Such a transition might also occur for the interstellar wind at a possible heliospheric bow shock (BS; cf. McComas et al. 2012); the heliopause (HP) is the boundary layer separating the LISM and the solar wind. The layer between the TS and the HP is called the inner heliosheath (IHS, light gray region in Figure 1), while the layer between the HP and a possible BS is called the outer heliosheath (OHS). The structure of the OHS became the subject of several investigations, triggered by recent observations of the *Interstellar Boundary Explorer* (*IBEX*) mission (cf. McComas et al. 2009, 2012).

The heliosphere is a protective shield against Galactic cosmic rays (GCRs). These highly energetic particles enter it at the HP and encounter the outward-flowing solar wind plasma, which carries a turbulent magnetic field that on average can be approximated by an Archimedean spiral. On their passage through the heliosphere the GCRs undergo modulation (e.g., McDonald 1998; Scherer et al. 2006; Potgieter 2011) such that their spectra measured at Earth are different from the spectrum at the outer boundary, the local interstellar spectrum (LIS). Lacking a way to directly measure this LIS in situ, several parameterizations of the proton LIS were developed with the help of galactic propagation models or derived indirectly from measurements at Earth, four of which will be investigated subsequently: Usoskin et al. (2005, US05), Garcia-Munoz et al. (1975, GM75), Webber & Higbie (2003, WH03), and Langner & Potgieter (2004, LA04).

In order to compare the various LIS models with the measurements at Earth's orbit, a full solution of Parker's transport equation (Parker 1965) is required, for which knowledge of the spatial, temporal, and rigidity dependence of all parameters involved in the modulation of GCRs as well as the size of the modulation volume is needed. The LIS enters such transport models as an outer boundary condition.

This overall picture was changed in the last few years not only from the data point of view, but also by numerical simulations: on the one hand the *Voyager 1* and *2* spacecraft crossed the TS on 2004 December 16 (at 94 AU) and 2008 July 31 (at 84 AU), respectively. Webber & Higbie (2009, WH09) derived a new LIS from these measurements in the IHS (Stone et al. 2005, 2008), which, as will be shown later, lies over the entire energy range below the four LIS models mentioned above. On the other hand, Scherer et al. (2011) used a simplified modulation model in order to demonstrate that the particles detected in the OHS are modulated rather than to represent the LIS. In consequence, the boundary value at the HP in modulation studies is a modulated heliopause spectrum (HPS) rather than the LIS, which instead is applicable farther out, e.g., at a possible BS. Combining these two results, we conclude that the LIS by Webber & Higbie (2009) can be regarded as such an HPS, and that the transport parameters in the OHS (i.e., the diffusion coefficient in a simplified approach) can be estimated by comparing the modulated LIS models with this spectrum. Moreover, they have to be compatible with the HPS in the sense that they fit to the HPS for reasonable diffusion coefficients. The goal of our investigations is to compare the OHS modulation for the four LIS models and to discuss possible consequences rather than to develop a new modulation model. For this reason, we use the simplified approach by Scherer et al. (2011) and validate our modulation spectra with their results.

Figure 2 shows the relative intensities of the LIS from US05 (black), GM75 (red), LA04 (blue), and WH09 (orange) normalized to the spectrum of WH03 (green), revealing significant

[3] Now at MINT-Kolleg, Universität Stuttgart, D-70174 Stuttgart, Germany.

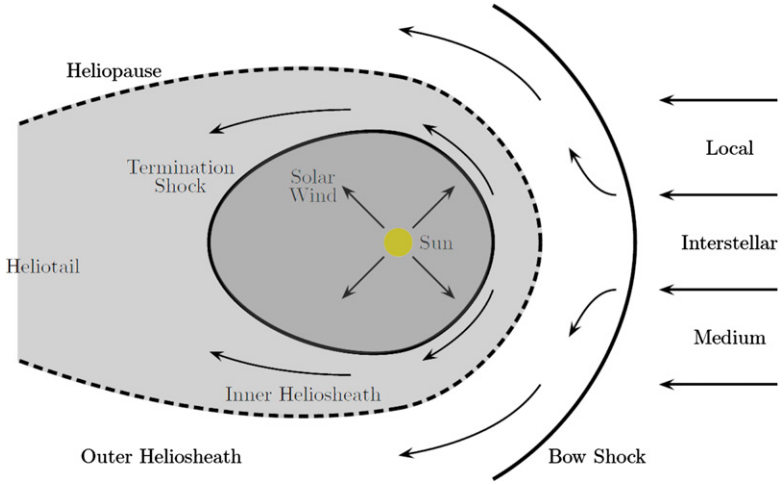

Figure 1. Projection of the heliosphere onto the equatorial plane, showing the streaming of the LISM from the right toward the Sun. The charged plasma interacts with the expanding solar wind and forms three discontinuities: the termination shock, the heliopause, and possibly a bow shock. This structure has so far been investigated by the two *Voyager* spacecraft, which are currently approaching the heliopause (adapted from Fichtner & Scherer 2000).

(A color version of this figure is available in the online journal.)

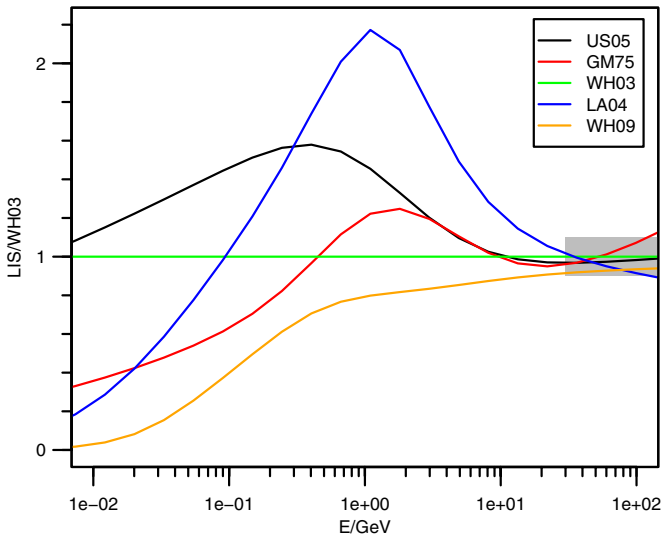

Figure 2. Relative intensities of the different LIS models investigated here with respect to the spectrum by Webber & Higbie (2003, WH03), illustrating the differences between the spectra and especially the problem that all spectra deviate from each other at energies above several 10 GeV, where hardly any modulation is expected, indicated by a tolerance interval of ±10% around the WH03 spectrum.

(A color version of this figure is available in the online journal.)

variations over the entire energy range, in particular also at energies above several of tens of GeV, where no modulation is expected. The figure, moreover, reveals that the LIS by Webber & Higbie (2009) is the lowest spectrum over the entire energy range. As mentioned above, this may be seen as consistent with the findings by Scherer et al. (2011) that the *Voyager* spacecraft measured a modulated HPS, rather than the LIS.

The amount of modulation required to "map" the four LIS models to the HPS must be computed numerically by solving Parker's transport equation (Parker 1965):

$$\frac{\partial j}{\partial t} = -\left(\boldsymbol{v}_{\rm sw} + \langle \boldsymbol{v}_d \rangle\right) \cdot \nabla j + \nabla \cdot \left(\mathbf{K}_S \cdot \nabla j\right) + \frac{1}{3}\left(\nabla \cdot \boldsymbol{v}_{\rm sw}\right) \frac{\partial}{\partial E}\left(\Gamma E j\right),$$

with j representing the differential intensity that is related to the CR distribution function f by $j = P^2 f$, where P is the particle rigidity. $\boldsymbol{v}_{\rm sw}$ is the solar wind velocity, $\langle \boldsymbol{v}_d \rangle$ represents the mean drift velocity, while $\mathbf{K}_S$ is the diffusion tensor. The factor Γ is given by $\Gamma = (E + 2E_0)/(E + E_0)$, where E is the kinetic energy of the particle and E_0 its rest energy (cf. Strauss et al. 2011). The modulation process is studied by means of numerical simulations with stochastic diffusion equations (SDEs). Like Scherer et al. (2011), we use the numerical propagation code by Strauss et al. (2011; see also Kopp et al. 2012). The physical model is based on Potgieter (1996), the essential parts of which are given in the Appendix. Like Scherer et al. (2011), we merely vary the value of the diffusion coefficient in the OHS, which can be either constant or proportional to the rigidity—scenarios which reflect two extreme cases (cf. Büsching & Potgieter 2008; Sternal et al. 2011).

The term $1/3\,(\nabla \cdot \boldsymbol{v}_{\rm sw})\,\partial/\partial E\,(\Gamma E j)$ in the transport equation represents the adiabatic energy change within the TS due to the divergence of the expanding solar wind. Because of the dependency of this term on the variation of j (and thus on the LIS as its outer boundary condition) with energy, the various LIS models undergo different modulation. Scherer et al. (2011) demonstrated that the adiabatic energy change (under the present model assumptions always cooling) is the dominating effect responsible for the modulation in the OHS. This is illustrated further in Figure 3 (cf. also Figure 4 of Scherer et al. 2011), where the energy change (in arbitrary units) of two sample trajectories of GCR protons for constant diffusion coefficients of $\kappa = 10^{27}$ cm^2 s^{-1} (left panel) and $\kappa = 10^{25}$ cm^2 s^{-1} (right panel) in the OHS are shown. The numerical code calculates the particle trajectories backward, i.e., the (pseudo) particle starts at the HP (red point) and leaves the system when it penetrates the (possible) BS (green point). The physical particle, thus, enters the heliosphere at the green point and is detected at the red one (cf. Kopp et al. 2012 for a discussion of forward/backward methods).

2. ANALYSIS AND DISCUSSION

2.1. The Diffusion Coefficient in the OHS

The modulated spectra resulting from our SDE simulations for the four LIS are shown in Figures 4 and 5 with OHS diffusion

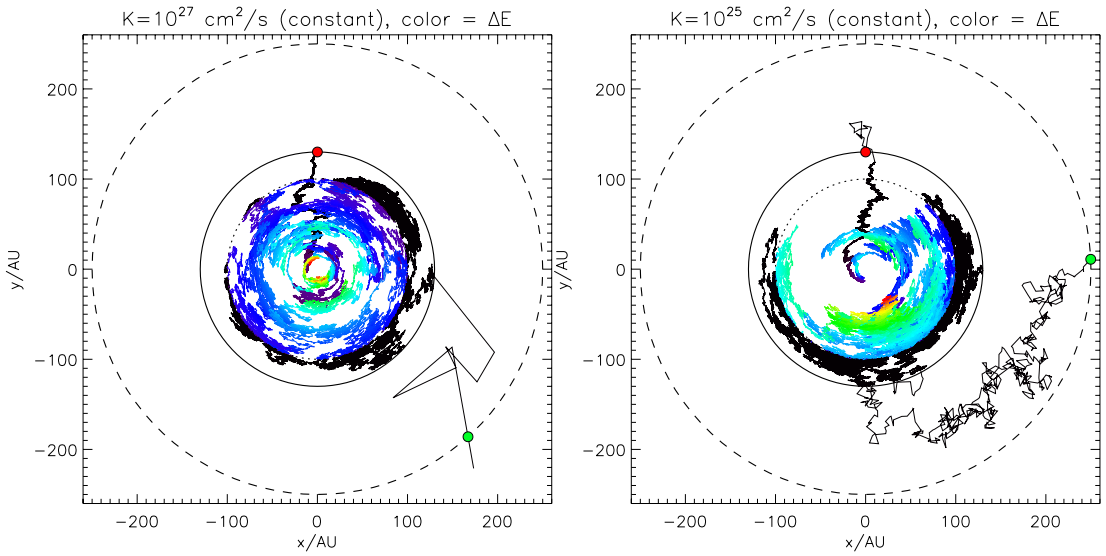

Figure 3. Sample trajectories of protons illustrating the OHS modulation due to adiabatic cooling within the TS for OHS diffusion coefficients of $\kappa = 10^{27}$ cm^2 s^{-1} (left panel) and $\kappa = 10^{25}$ cm^2 s^{-1} (right panel). The particles enter the heliosphere at a possible BS (green point), propagate through the heliosphere, undergo adiabatic cooling inside the TS, and finally penetrate the HP at the red point. The color indicates the energy loss (in arbitrary units) on a scale ranging from black (no energy loss) over blue and green to red. The dotted lines represent the TS, the solid ones show the HP, while the dashed lines represent the boundary of the computational volume.

(A color version of this figure is available in the online journal.)

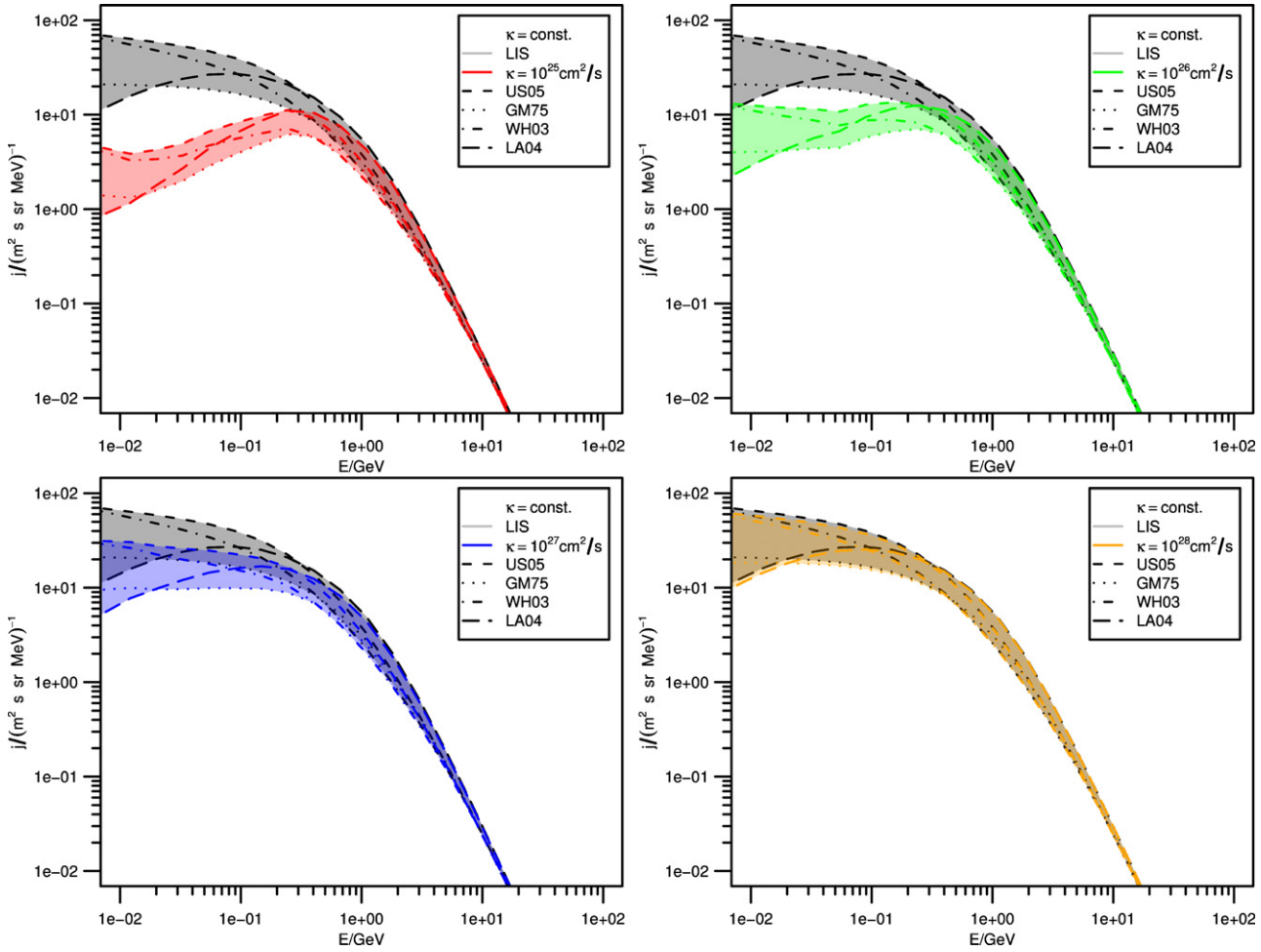

Figure 4. Colored bands show the modulated spectra for a constant diffusion coefficient κ in the OHS for the four LIS models by US05 (short dashes), GM75 (dotted), WH03 (dash-dotted), and LA04 (long dashes), with the upper left panel showing the simulation results for $\kappa = 10^{25}$ cm^2 s^{-1} (red), the upper right panel for $\kappa = 10^{26}$ cm^2 s^{-1} (green), the lower left panel for $\kappa = 10^{27}$ cm^2 s^{-1} (blue), and the lower right panel for $\kappa = 10^{28}$ cm^2 s^{-1} (orange). In all four panels the LIS themselves are represented by the gray bands.

(A color version of this figure is available in the online journal.)

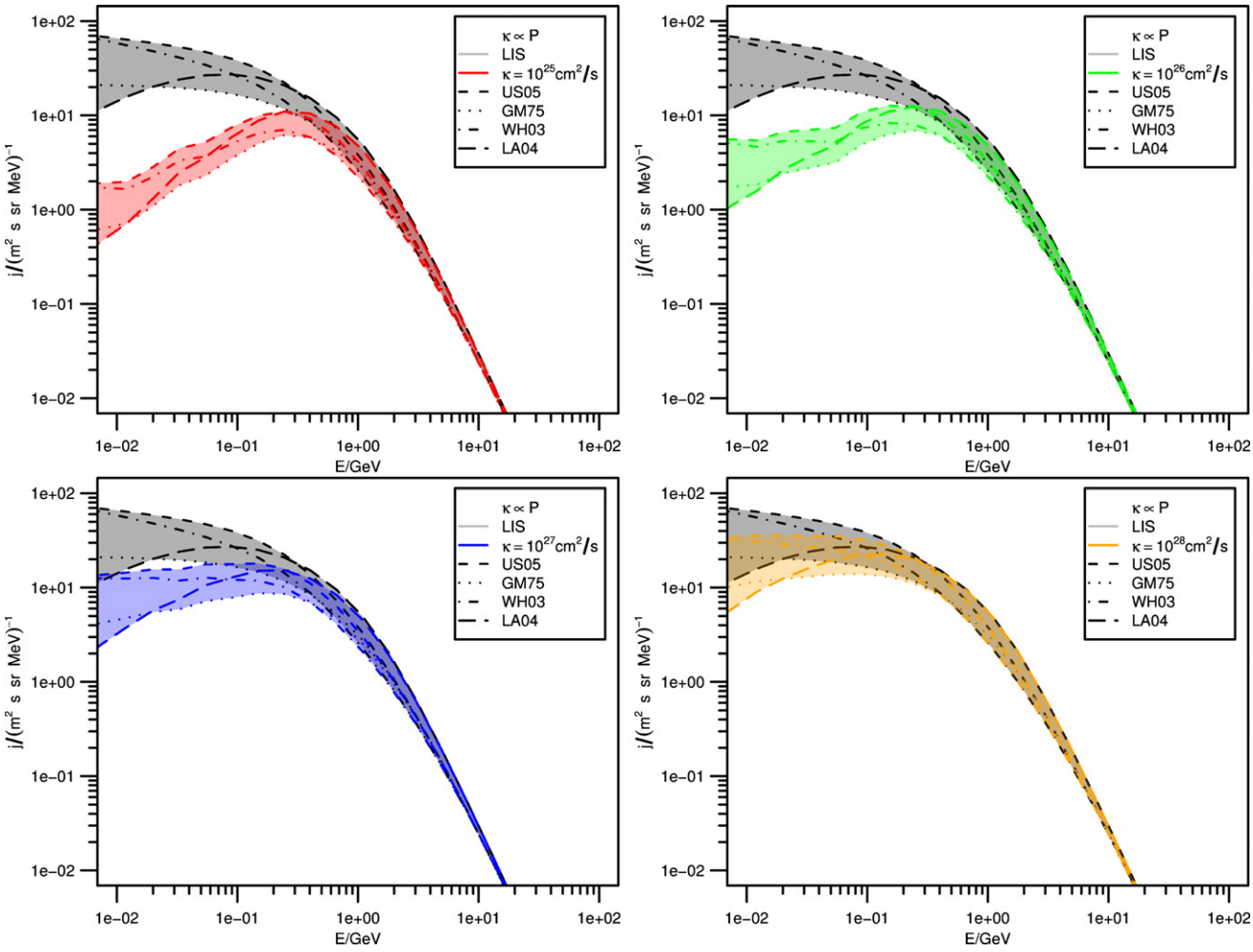

Figure 5. Same as Figure 4 but for energy-dependent diffusion ($\kappa \propto P$) in the OHS.

(A color version of this figure is available in the online journal.)

coefficients κ being constant and proportional to the particle rigidity, respectively. While the line style stands for the LIS model (US05: short dashes, GM75: dotted, WH03: dash-dotted, and LA04: long dashes), the color represents the value of the diffusion coefficient in the OHS: $\kappa = 10^{25}$ (red, upper left panel), $\kappa = 10^{26}$ (green, upper right panel), $\kappa = 10^{27}$ (blue, lower left panel), and $\kappa = 10^{28}$ (orange, lower right panel). Furthermore, in all four panels gray stands for the LIS itself. The colored bands indicate the range covered by all four LIS models together: the upper boundary is formed by the spectra of US05 (0.01–0.3 GeV) and LA04 ($E > 0.3$), and the lower one by the spectra of LA04 ($E < 0.02$ GeV), GM75 (0.02–0.4 GeV), and WH03 ($E > 0.4$ GeV). As expected, the modulation decreases with increasing κ, so that it nearly vanishes for $\kappa = 10^{28}$ cm^2 s^{-1} and is stronger at lower energies for the case $\kappa \propto P$. The bands show in both cases a widening toward lower energies.

2.2. Estimation of the Diffusion Coefficient in the Outer Heliosheath

We estimate the diffusion coefficient κ in the OHS by comparing the modulated spectra shown in Figures 4 and 5 with the "measured" HPS by Webber & Higbie (2009). Figure 6 shows the bands displayed in Figures 4 and 5 in the left and right panels, respectively, together with the WH09 spectrum (black line). Although for lower energies the HPS lies in a reasonable κ range between 10^{26} (green) and 10^{27} cm^2 s^{-1} (blue), the simulation results as well as the unmodulated LIS models themselves exceed the HPS in the high-energy range above several 10 GeV, where essentially no modulation should be present. Allowing for a tolerance of ±10 % around the LIS model by WH03 (gray area in Figure 2) we shift the HPS by Webber & Higbie (2009), which is essentially at the lower end of this area, upward by 10% and 20%. The result is shown in Figure 7, where only the two relevant modulation bands for $\kappa = 10^{26}$ cm^2 s^{-1} (green) and 10^{27} cm^2 s^{-1} (blue) are shown. The HPS is represented again by the solid line, while the HPS being shifted upward by 10% and 20% are depicted by long and short dashes, respectively. As in Figure 6, the left panel shows the case of constant κ, the right one that of $\kappa \propto P$ in the OHS. It follows

1. If we permit that the spectrum proposed by Webber & Higbie (2009) may be shifted upward by 10% to 20%, all four modulated LIS models investigated in this study are consistent with the (modulated) HPS.
2. The diffusion coefficient in the OHS can be estimated to a few $\kappa = 10^{26}$ up to $\kappa = 10^{27}$ cm^2 s^{-1}.

Because the colored bands in Figure 7 cover all four LIS models including possible refinements of the models, none of them can be excluded due to the *Voyager* measurements, and, moreover, we conclude that the *Voyager* spacecraft will not measure the "true" LIS, but a modulated spectrum with a diffusion coefficient

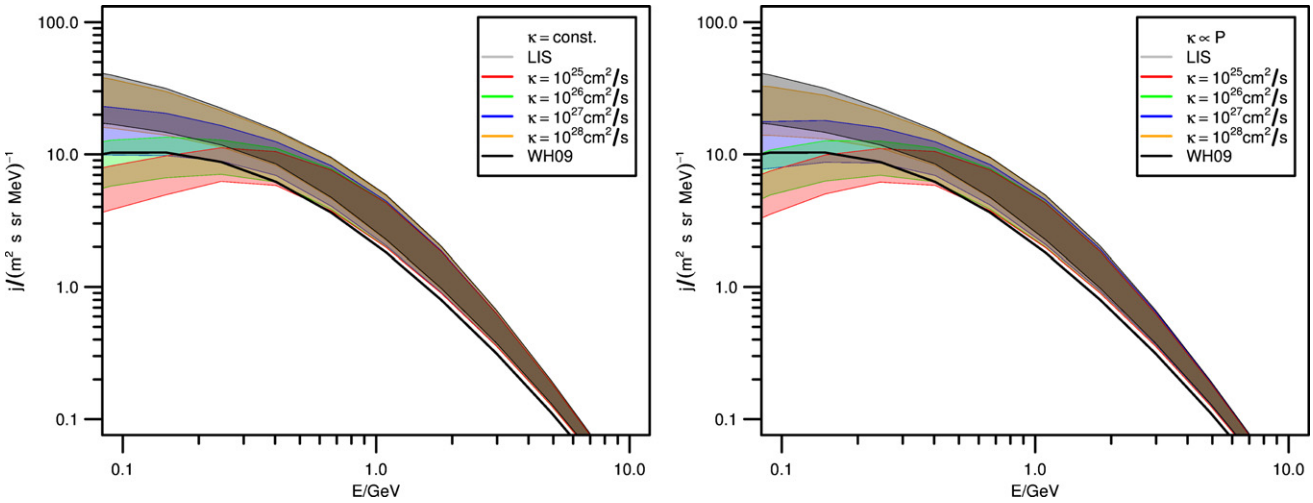

Figure 6. Combination of our simulations for a constant (left panel) and a rigidity-dependent (right panel) diffusion coefficient. The colored bands are taken from Figures 4 and 5; the HPS by Webber & Higbie (2009) is displayed as the black line.

(A color version of this figure is available in the online journal.)

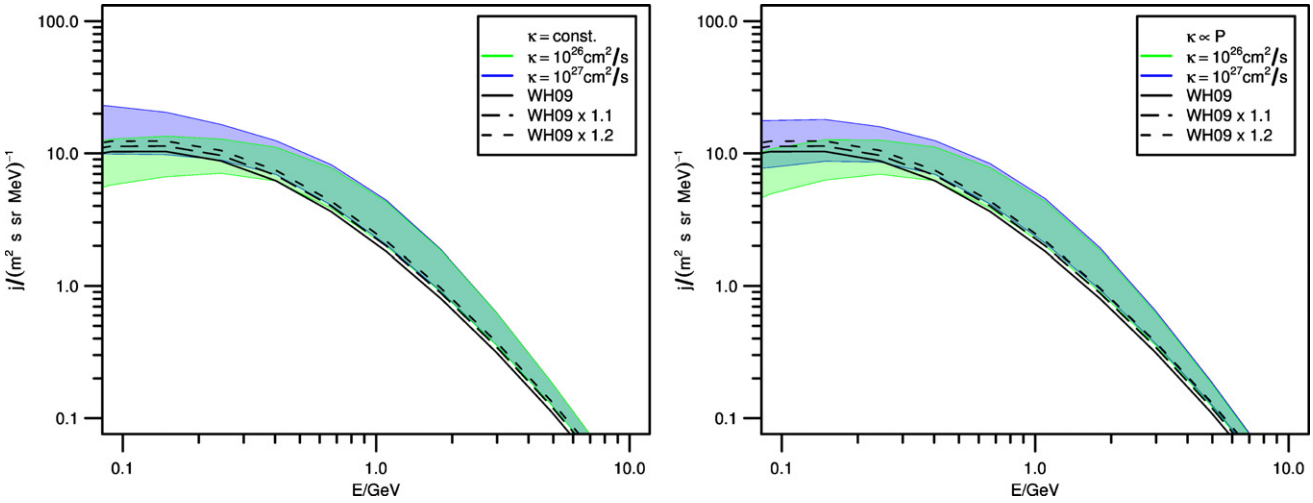

Figure 7. Bands for $\kappa = 10^{26}$ cm^2 s^{-1} (green) and $\kappa = 10^{27}$ cm^2 s^{-1} (blue) are shown together with the HPS (solid line), which was shifted up by factors of 10% (long-dashed lines) and 20% (short-dashed lines) within the "tolerance" area in Figure 2 in order to account for deviations of the LIS models above 10 GeV, where no modulation should occur.

(A color version of this figure is available in the online journal.)

in the range given above. For access to further information on the LIS, we will lead to wait for a dedicated space mission like the *Interstellar Probe* (*ISP*).

Another line was followed by Herbst et al. (2010) who studied the variation of the so-called modulation parameter, a proxy for solar activity, with the different LIS models. In order to do so, they investigated the value of this quantity during grand solar minima derived from measurements of the cosmogenic radionuclide ^{10}Be in terrestrial archives like ice cores. In this approach, they found that the spectra by GM75 and WH03 as well as the HPS by WH09 lead to negative modulation parameters during such periods of time, corresponding to a modulated spectrum at Earth exceeding the LIS. All four LIS models, except perhaps the very low spectrum by Webber & Higbie (2009), are consistent with recent ^{10}Be data, reflecting the solar activity over the last centuries. In the still simple, but more elaborate approach used in the present study, such minimum conditions would correspond to a diffusion coefficient above several 10^{27} or 10^{28} cm^2 s^{-1}, leading to mean free paths large enough to cause almost negligible diffusion in the OHS.

3. SUMMARY AND CONCLUSIONS

In this paper, we used numerical simulations with the SDE approach by Strauss et al. (2011) and Kopp et al. (2012) to compute and compare the modulated spectra in the OHS for the four LIS models by Usoskin et al. (2005), Garcia-Munoz et al. (1975), Webber & Higbie (2003), and Langner & Potgieter (2004). A fifth LIS model was derived by Webber & Higbie (2009) from recent *Voyager* measurements and lies below the other four LIS models over the entire energy range. Motivated by the findings by Scherer et al. (2011), who demonstrated that modulation already occurs in the OHS instead of at the HP, we concluded that this spectrum is a modulated HPS rather than the "true" LIS. By comparing the four modulated LIS spectra with this HPS we can estimate the diffusion coefficient to lie in the range between a few 10^{26} and 10^{27} cm^2 s^{-1}. Since all four LIS models are, thus, compatible with the *Voyager* data, none of them can be excluded. Since *Voyager* obviously detected a modulated spectrum rather than the LIS, there will be no way to measure LIS in the near future. Only a dedicated mission like, e.g., the *ISP* can be expected to do so.

The boundary conditions for the proper choice of the LIS, although no simple way to derive the LIS exists, may, however, come from the other end of the modulation chain: the results by Herbst et al. (2010) indicate that some of the LIS models are not consistent with the data of cosmogenic radionuclides in so far as the modulated spectra at Earth would exceed the LIS during grand solar minima. These findings, however, are based on the use of simplifying proxies for solar activity, such that a fully self-consistent model chain (e.g., Scherer et al. 2006; McCracken 2007) is probably required to learn more about the LIS.

We thank Du Toit Strauss and Marius S. Potgieter for numerous productive discussions as well as providing the numerical SDE code for our investigations.

APPENDIX

THE MODEL

The model is essentially based on Potgieter (1996); the values are the same as in Scherer et al. (2011). The TS is located at 100 AU, the HP at 130 AU, and a possible BS forms the outer boundary of the simulation volume at 250 AU. Within the HP, the solar wind speed is assumed to be directed radially outward with a constant value of 400 km s^{-1}, beyond which the solar wind speed is assumed to vanish. The adiabatic energy change due to the factor $\nabla \cdot \boldsymbol{v}_{\rm sw} = 2(v_{\rm sw}/r)$ is taken into account only for $r \leqslant r_{\rm TS}$ and is set to zero elsewhere. The mean free path is given by

$$\lambda_{\parallel} = \lambda_0 \cdot (1 + r) \cdot P, \tag{A1}$$

with $\lambda_0 = 0.1$ for distances between $r \leqslant r_{\rm TS}$ and 0.01 beyond. Within the HP the diffusion tensor is

$$\mathbf{K}_S = \begin{pmatrix} \kappa_{\rm rr} & 0 & \kappa_{r\varphi} \\ 0 & \kappa_{\vartheta\vartheta} & 0 \\ \kappa_{\varphi r} & 0 & \kappa_{\varphi\varphi} \end{pmatrix} \tag{A2}$$

with the components

$$\begin{aligned} \kappa_{\rm rr} &= \kappa_{\parallel} \cdot \cos^2\psi + \kappa_{\perp,r} \cdot \sin^2\psi \\ \kappa_{r\varphi} &= (\kappa_{\perp,r} - \kappa_{\parallel}) \cdot \sin\psi \cdot \cos\psi = \kappa_{\varphi r} \\ \kappa_{\vartheta\vartheta} &= \kappa_{\perp,\vartheta} \\ \kappa_{\varphi\varphi} &= \kappa_{\parallel} \cdot \sin^2\psi + \kappa_{\perp,r} \cdot \cos^2\psi, \end{aligned} \tag{A3}$$

where ψ represents the Parker angle between the radial direction and that of the averaged heliospheric magnetic field (HMF) at the actual position of the particle, and the components are related to the mean free path by

$$\begin{aligned} \kappa_{\parallel} &= \frac{1}{3}\lambda_{\parallel}\, v \\ \kappa_{\perp,r} &= \kappa_{\perp,\vartheta} = \kappa_0 \cdot \kappa_{\parallel}, \end{aligned} \tag{A4}$$

with v representing the speed of the particle and $\kappa_0 = 0.1$. Note the change of $\lambda_{\parallel}$ beyond the TS according to Equation (A1).

Beyond the HP the diffusion tensor is replaced by a scalar value, which is varied between 10^{25} and 10^{28} cm^2 s^{-1}, and is either constant or proportional to the rigidity P. This model neglects drift effects and, moreover, does not take into account the heliospheric current sheet; for the inclusion of these effects we refer to Strauss et al. (2012).

REFERENCES

Büsching, I., & Potgieter, M. S. 2008, Adv. Space Res., 42, 504
Fichtner, H., & Scherer, K. 2000, in The Outer Heliosphere: Beyond the Planets, ed. K. Scherer, H. Fichtner, & E. Marsch (Katlenburg-Lindau: Copernicus-Gesellschaft), 1
Garcia-Munoz, M., Mason, G. M., & Simpson, J. A. 1975, ApJ, 202, 265
Herbst, K., Kopp, A., Heber, B., et al. 2010, J. Geophys. Res., 115, D00I20
Kopp, A., Büsching, I., Strauss, R. D., & Potgieter, M. S. 2012, Comput. Phys. Commun., 183, 530
Langner, U. W., & Potgieter, M. S. 2004, J. Geophys. Res., 109, A01103
McComas, D. J., Alexashov, D., Bzowski, M., et al. 2012, Science, 336, 1291
McComas, D. J., Allegrini, F., Bochsler, P., et al. 2009, Science, 326, 959
McCracken, K. G. 2007, Adv. Space Res., 40, 1070
McDonald, F. B. 1998, Space Sci. Rev., 83, 33
Parker, E. N. 1965, Planet. Space Sci., 13, 9
Potgieter, M. S. 1996, J. Geophys. Res., 101, 24411
Potgieter, M. S. 2011, Space Sci. Rev., 1
Scherer, K., Fichtner, H., Borrmann, T., et al. 2006, Space Sci. Rev., 127, 327
Scherer, K., Fichtner, H., Strauss, R. D., et al. 2011, ApJ, 735, 128
Sternal, O., Engelbrecht, N. E., Burger, R. A., et al. 2011, ApJ, 741, 23
Stone, E. C., Cummings, A. C., McDonald, F. B., et al. 2005, Science, 309, 2017
Stone, E. C., Cummings, A. C., McDonald, F. B., et al. 2008, Nature, 454, 71
Strauss, R. D., Potgieter, M. S., Büsching, I., & Kopp, A. 2012, Astrophys. Space Sci., 339, 223
Strauss, R. D., Potgieter, M. S., Kopp, A., & Büsching, I. 2011, J. Geophys. Res., 116, 12105
Usoskin, I. G., Alanko-Huotari, K., Kovaltsov, G. A., & Mursula, K. 2005, J. Geophys. Res., 110, A12108
Webber, W. R., & Higbie, P. R. 2003, J. Geophys. Res., 108, 1355
Webber, W. R., & Higbie, P. R. 2009, J. Geophys. Res., 114, A02103